High-bandwidth polarimeter for a high density, accelerated spheromak

ARTICLE *in* THE REVIEW OF SCIENTIFIC INSTRUMENTS · AUGUST 2013

Impact Factor: 1.61 · DOI: 10.1063/1.4819307 · Source: PubMed

3 AUTHORS, INCLUDING:

Patrick JF Carle

General Fusion Inc.

9 PUBLICATIONS **35** CITATIONS

SEE PROFILE

Stephen James Howard

General Fusion Inc.

50 PUBLICATIONS **69** CITATIONS

SEE PROFILE

AIP | Review of Scientific Instruments

High-bandwidth polarimeter for a high density, accelerated spheromak

Patrick J. F. Carle, Stephen Howard, and Jordan Morelli

Citation: Rev. Sci. Instrum. **84**, 083509 (2013); doi: 10.1063/1.4819307
View online: http://dx.doi.org/10.1063/1.4819307
View Table of Contents: http://rsi.aip.org/resource/1/RSINAK/v84/i8
Published by the AIP Publishing LLC.

High-bandwidth polarimeter for a high density, accelerated spheromak

Patrick J. F. Carle,[1] Stephen Howard,[2,a)] and Jordan Morelli[1]
[1]*Department of Physics, Queen's University, 99 University Ave., Kingston, Ontario K7L 3N6, Canada*
[2]*General Fusion, Inc., 108-3680 Bonneville Pl, Burnaby, British Columbia V3N 4T5, Canada*

(Received 16 July 2013; accepted 12 August 2013; published online 26 August 2013)

A three-beam heterodyne polarimeter has been built to diagnose the PI-1 plasma injector at General Fusion, Inc. The polarimeter measures plasma density and Faraday rotation, which can provide estimates of magnetic field magnitude and direction. Two important calibration steps are required for the polarimeter to produce reasonable Faraday rotation signals. Beam polarization ellipticity must be measured to ensure there is a linear Faraday rotation response. In addition, the two beams travelling through the plasma must be collinear to reduce error due to differences in plasma density. Once calibrated, the Faraday rotation signals are in much better agreement with other diagnostics. For a null signal, the Faraday rotation measurement noise floor is 0.1° at 0.5 MHz bandwidth. Comparing preliminary spheromak Faraday rotation measurements to a model, the maximum error is about 0.3° at 0.5 MHz bandwidth, which is primarily due to electrical noise during the injector's capacitor discharge and limitations of the model. At a bandwidth of 0.5 MHz, the polarimeter has an axial resolution between 6 cm and 30 cm depending on the speed of the spheromak, which varies between 30 km/s and 150 km/s. The spheromak length ranges from 0.75 m to 2 m. Additional polarimeter chords will be added in future upgrades. © *2013 AIP Publishing LLC*. [http://dx.doi.org/10.1063/1.4819307]

I. INTRODUCTION

General Fusion, Inc. (GF) is working towards building a prototype magnetized target fusion generator[1,2] in which a plasma injector (see Figure 1) forms and accelerates a spheromak plasma[3,4] into a reactor chamber. As the spheromak accelerates, the tapered injector electrodes compress the plasma to higher density and temperature. The spheromak would then be compressed to fusion conditions using an acoustically driven implosion of a liquid metal liner. Two plasma injectors, PI-1 and PI-2, have been built and are undergoing tests to generate an optimized plasma.

The injectors are equipped with a number of diagnostics to measure plasma parameters. The Thomson scattering system can read temperature at a single point and time. Ion Doppler spectroscopy gives time-resolved, average temperature. A single-exposure survey spectroscopy system displays line radiation over a broad spectrum. Infrared-wavelength interferometers measure line-averaged density along a chord. Rogowski coils monitor current through the injector electrodes. Surface magnetic probes and insertable three-axis probe arrays resolve the magnetic field.

With this suite of diagnostics, it is possible to use density and magnetic field measurements to constrain models of the spheromak's magnetic geometry and dynamics. Magnetic field measurements are typically obtained with probes.[5] To obtain information on the plasma core, probes must be immersed inside the plasma. Towards the end of the injector, the spheromak can reach temperatures in the hundreds of eV with densities of 10^{22} m^{-3}. Such harsh conditions could severely damage immersed probes, contaminate the injector vacuum and perturb the plasma.[6]

In this way, a non-perturbing magnetic field diagnostic like the polarimeter is a useful alternative. A particularly difficult and novel challenge for GF's polarimeter is to resolve a plasma that is about 1 m long as it is accelerated to speeds on the order of 100 km/s. This requires a high measurement bandwidth to obtain an axial profile of the passing plasma. A bandwidth of 1 MHz could provide measurements with axial resolution on the order of 10 cm.

This paper describes the polarimeter built to diagnose plasmas in the GF injector. Section II reviews the three-beam heterodyne polarimetry approach. The experimental setup is detailed in Sec. III. In Secs. IV–VI, noise sources and calibration steps are described. Preliminary results are given in Sec. VII and a summary in Sec. VIII.

II. PLASMA POLARIMETRY

The polarization plane of a linearly polarized beam of light can be rotated when passing through a magnetized plasma. This effect is known as Faraday rotation.[7] Since a linearly polarized beam is equivalent to the superposition of a left and right circularly polarized beam, the left or right-handed beam, respectively, sees a higher or lower refractive index and therefore an advance or lag in phase. The Faraday rotation, ϕ_f, can be defined as half the phase difference between the left and right-handed beams.[8] It depends on beam wavelength, λ, plasma electron density, n_e, and magnetic field, $\mathbf{B}$

$$\phi_f[\text{rad}] = 2.63 \times 10^{-13}\lambda^2 \int n_e \mathbf{B} \cdot \mathbf{dl}, \tag{1}$$

where $\mathbf{dl}$ is an infinitesimal vector in the direction of the beam's path through the plasma. Therefore, the Faraday rotation depends only on the component of magnetic field parallel to the beam direction, $B_\parallel$.

a)URL: www.generalfusion.com.

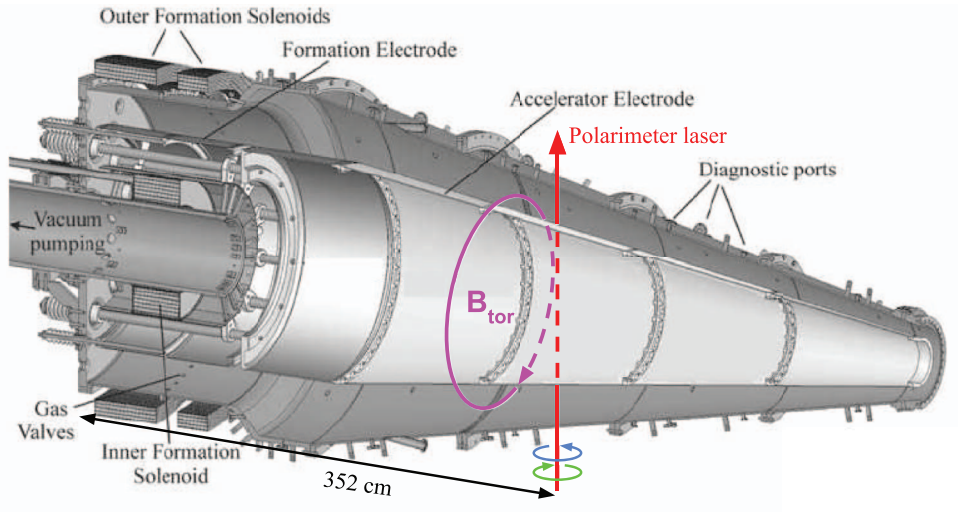

FIG. 1. PI-1 plasma injector with polarimeter laser chord at the 352 position. Laser passes in between inner and outer electrodes.

An additional phase shift, ϕ_n, due to the change in the plasma's refractive index with plasma density, is incurred independent of the polarization state[9]

$$\phi_n[\text{rad}] = -2.82 \times 10^{-15}\lambda \int n_e dl. \tag{2}$$

A polarimeter can measure these phase shifts to obtain estimates of plasma magnetic field and density. An implementation that is robust to noise and minimizes the number of required detectors is the three-beam heterodyne method[10–12] depicted in Figure 2.

The system uses three primary beams (ω_1, ω_2, ω_3) split from a CO_2 laser that outputs a linearly (vertically) polarized beam. Two of the three beams, ω_1 and ω_2, are frequency up-shifted by 25 MHz and 40 MHz acousto-optic modulators (AOMs). The AOMs do this by effectively reflecting the beams off acoustic waves, which Doppler shifts the beams.

As shown in Figure 3, beam ω_1 is sent through a $\lambda/2$ waveplate, which changes its linear polarization from vertical to horizontal. Beams ω_1 and ω_2 are then combined with a thin film polarizer (TFP) to divert most of the power into a single combined beam. The combined beams are then reflected off a phase retarding reflector (PRR), which converts linear to circular polarization and vice versa. Before hitting the PRR, the beams' polarization planes are perpendicular to one another. This causes the PRR to create circularly polarized beams of opposite handedness (i.e., ω_1 is left-circularly polarized and ω_2 is right-circularly polarized). Therefore, when sent through a magnetized plasma, beams ω_1 and ω_2 are, respectively, phase shifted by $\phi_n + \phi_f$ and $\phi_n - \phi_f$.

Once through the plasma, the beams ω_1 and ω_2 are combined with beam ω_3 using a 50/50 beam splitter. The beams are then sent through a TFP to select a single electric field component (i.e., vertical), and focussed onto a detector. When the three beams are interfered, they produce a heterodyne signal composed of the beams' beat frequencies: 15 MHz, 25 MHz, and 40 MHz. The 15 MHz beat signal between beams ω_1 and ω_2 has a phase shift that is the difference between the two interfering beams: $2\phi_f$. This gives the Faraday rotation through the plasma, and an estimate of the internal magnetic field if the density is known. The interference of the plasma beams with beam ω_3, which does not pass through the plasma, gives plasma density. The two beat signals produced at 25 MHz and 40 MHz contain a phase shift of $\phi_n \pm \phi_f \approx \phi_n$ since $\phi_n \gg \phi_f$. The phase shifts from these beat signals are extracted with a demodulation algorithm by comparing them to reference beat signals.[13]

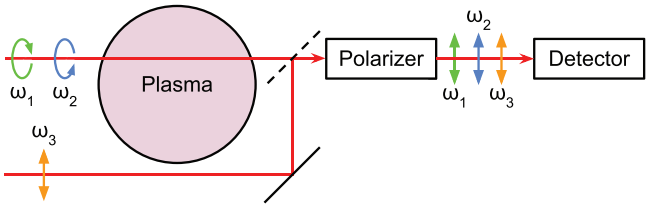

FIG. 2. Three-beam heterodyne polarimeter used at GF.

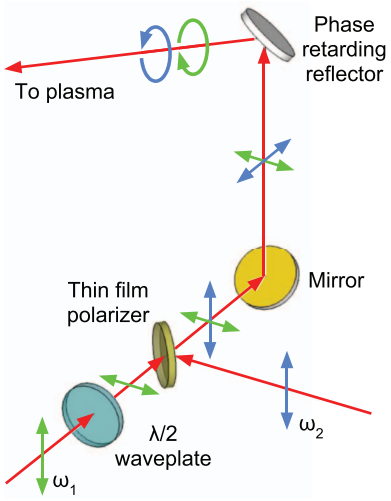

FIG. 3. Polarimeter beam combination and conversion to circular polarization.

III. EXPERIMENTAL SETUP

A CO_2 laser (Access Laser Merit-S) is used, which outputs an 8 W, 10.6 μm, linearly polarized beam. At 10.6 μm, the beam's frequency is an order of magnitude greater than the plasma frequency assuming a peak density of 10^{23} m^{-3}. Therefore, reflection off the plasma should not be a concern. As mentioned previously, the two AOMs (Brimrose GEMF-40-4-10.6 and Brimrose GEMF-25-4-10.6) produce frequency shifts of 25 MHz and 40 MHz giving interference beat signals at 15 MHz, 25 MHz, and 40 MHz. The peaks are separated by at least 10 MHz, allowing for measurement bandwidths on the order of a MHz. The detector is a non-cooled HgCdTe detector (Vigo PVM-10.6) with AC-coupled pre-amplifier. The signal is sampled at 125 MS/s with a 12-bit Picoscope 4227 digitizer.

The polarimeter is located about halfway down the PI-1 plasma injector at the 352 position (i.e., 352 cm away from the injector back flange, see Figure 1). The vacuum vessel windows are anti-reflection coated ZnSe for high transmission of the 10.6 μm beam. The chord inside the plasma is vertical and 0.60 m long. Since this chord is tangential, the Faraday rotation depends in theory on both radial (component of the poloidal) and toroidal field. However, magneto-hydrodynamic (MHD) simulations and Grad-Shafranov equilibrium models have shown that the radial field contribution is small. Therefore, the polarity of the Faraday rotation should depend predominantly on the toroidal field, which is in the clockwise direction looking from the tip of the injector towards the back flange.

An insertable magnetic probe array was available on some shots to measure the magnetic field direction and magnitude. The probe array is located at the same axial position as the polarimeter chord. The linear array is enclosed in an alumina ceramic tube and contains five radial, five axial, and five toroidal probes spanning approximately 14 cm. Surface magnetic probes are located across the entire injector and are useful for measuring axial field to determine the position of the spheromak in the injector. Rogowski coils measure current flow through the injector electrodes, which is the predominant source of toroidal field.

IV. BEAM POLARIZATION

Ideally, both plasma beams should be perfectly circularly polarized when passing through the plasma in order to have a linear relationship between phase shift and observed Faraday rotation. Beams with strong elliptical polarization can produce phase shifts which suggest much larger or smaller Faraday rotation than is actually the case.

Beam polarization ellipticity is calibrated using a half-waveplate rotating[14] at 15 Hz. The plasma beams are sent through the rotating waveplate, which phase shifts the beams and emulates Faraday rotation in a magnetized plasma. A full Faraday rotation cycle is measured for every quarter rotation of the waveplate.

In the initial optics arrangement (Figure 4), two phase retarding mirrors each reflected one of the two plasma beams before they were combined. In principle, this setup could produce circularly polarized beams while avoiding the use of a half-waveplate. However, space constraints made it difficult to properly align the beams with respect to the PRRs. The result was a nonlinear response during polarization calibration as shown in Figure 5. The polarization ellipticity was sufficiently poor that it could have caused as much as a factor of 2 overestimation of the true Faraday rotation signal.

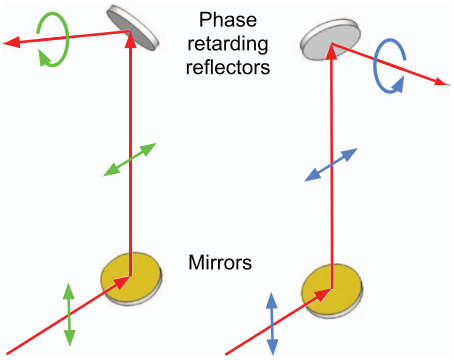

FIG. 4. Initial beam combination setup gave poorly circularly polarized beams due to difficulties in aligning the beams with respect to the PRRs.

The cause of the problem was determined to be at the plasma beams' conversion from linear to circular polarization with the phase retarding mirrors. A half-waveplate was placed into the system so that both plasma beams were combined before conversion to circular polarization (Figure 3). The result was a dramatic improvement in the linearity of the response as shown in Figure 5. Polarization ellipticity error has been reduced to less than 0.1°.

V. BEAM COLLINEARITY

Beam collinearity can also be a source of significant Faraday rotation error. If the plasma beams are not collinear, spatial variation of density can result in a difference of phase shifts between the two beams, $\Delta\phi_n$. This would distort the Faraday rotation phase shift measurement to $2\phi_f + \Delta\phi_n$. For $B_\parallel = 1$ T, the ratio ϕ_n/ϕ_f is about 1000, i.e., the ratio of Eq. (2) to Eq. (1). Therefore, the polarimeter is much more sensitive to density phase shifts than to Faraday rotation phase shifts along the same chord. For example, given the geometry at the 352 position, with $B_\parallel = 1$, a parabolic density profile with line average of 10^{22} m^{-3} and a beam misalignment of

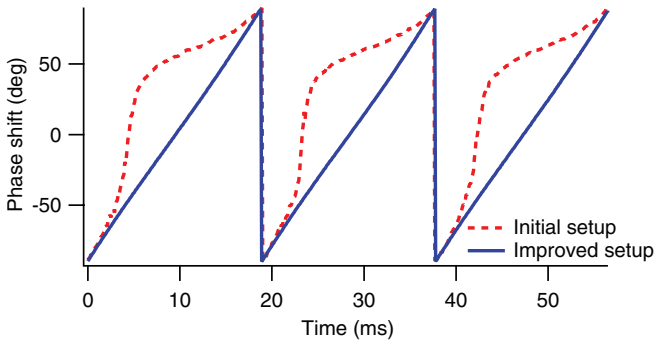

FIG. 5. Phase shift responses due to beam polarization ellipticity for different setups. Obtained using λ/2 waveplate rotating at about 15 Hz.

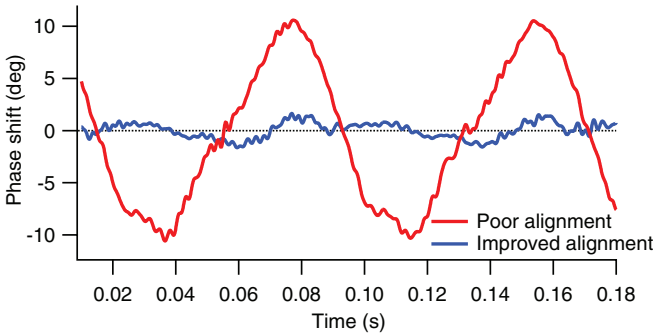

FIG. 6. Apparent Faraday rotation during beam alignment by placing a rotating, 14 arc min (0.23°) wedge of ZnSe in the path of the plasma beams. Both signals have bandwidths of 500 Hz. Signal sampled at 10.4 kHz.

0.1 mm, the density phase shift noise introduced into the Faraday rotation signal would be about 9°. The maximum Faraday rotation signal due to the interaction with the magnetic field would be about 8°. In this scenario, the desired signal could be washed out with a similarly shaped noise signal due to beam misalignment that is coincident with the arrival of the spheromak.

To eliminate this noise, the beams can be precisely aligned with a rotating wedge[15] of ZnSe placed along the path of the plasma beams. If the beams are not collinear, they will have slightly different path lengths in the wedge. Therefore, they will experience different phase shifts, which will appear in the Faraday rotation signal. To improve the collinearity of the beams, their positions can be adjusted by translating and angling them in order to eliminate the signal created from the rotating wedge. Figure 6 gives an example of the signal produced from the beam alignment process.

The wedge's rotation rate is limited to about 15 Hz. Given the polarimeter's standard sampling rate of 125 MHz, millions of samples are needed to collect a full rotation of the wedge. This slows computation time and makes it difficult to obtain instant feedback between adjusting the position of a beam and seeing the effect on alignment on a computer screen. However, when sampled below the Nyquist frequency, the frequency peak of interest will shift to a new frequency as a result of aliasing. Therefore, it is simply a matter of determining where this aliased peak is expected and changing the demodulation frequency in the algorithm accordingly. In this manner, a much lower sampling rate can be used, lowering the computational burden and easing the alignment process.

VI. OTHER NOISE SOURCES

To facilitate alignment, the polarimeter box is located a few metres from the vacuum vessel at the 352 position. Unfortunately, this places the box near the capacitor banks, which generate transient noise pulses during discharge that the equipment can pick up. To compensate, the laser, AOMs, and detection equipment are housed in a box with 1/8 in. thick aluminum walls. It is ensured the box is well-sealed and has a good connection to ground to act as a Faraday cage that can reflect much of the electromagnetic noise. In addition, just before a shot, the box is disconnected from the building power lines using a relay. During this short time, the equipment is powered with an uninterruptible power supply. Within the box, standard methods of shielding from radio-frequency (RF) noise are used such as carrying power and signals with shielded BNC cables and avoiding ground loops. These steps have significantly reduced capacitor discharge noise.

The vacuum vessel windows are made of 3 mm thick ZnSe, which has a high Verdet constant and can therefore cause a significant Faraday rotation at high magnetic fields. The Faraday rotation due to the windows is $\phi_f = V d B_\parallel$, where V is the Verdet constant, d the window thickness, and $B_\parallel$ the magnetic field parallel to the direction of the beam. The Verdet constant[16] for ZnSe at 10.5 μm is $V = 20 \pm 6°$ T^{-1} m^{-1}. The magnetic field at the windows is strongly attenuated since the windows are recessed in a 10 cm deep well. Therefore, an upper limit of $B_\parallel = 0.1$ T at the windows is chosen, though the true field at the windows is likely much less. For transmission through two windows with $V = 26°$ T^{-1} m^{-1}, the Faraday rotation due to the windows is 0.02°. Assuming plasma parameters along the polarimeter chord of $n_e = 10^{21}$ m^{-3} and $B = 0.5$ T, the Faraday rotation signal is 0.5°. The Faraday rotation from the laser passing through the plasma is over 20 times greater than that from the windows. Therefore, the windows have only a small effect on measurements.

The Cotton-Mouton effect,[17] which affects beam polarization ellipticity and depends on magnetic field perpendicular to the beam propagation direction, can also add noise into polarimeter measurements. However, for this experiment, the magnitude of the magnetic field and the beam wavelength are sufficiently low that the effect is negligible.

The noise floor for a null signal (i.e., no capacitors discharging, no plasma passing by) is about 0.1° for a 0.5 MHz bandwidth. The noise spectrum is white, suggesting the source is likely detector thermal noise. To improve the noise floor, the detectors could be cooled to lower the thermal noise or the beam power could be increased to boost the detector signal.

VII. RESULTS

Faraday rotation measurements can be compared to a Faraday rotation model generated with Eq. (1) using other diagnostics as inputs. The model assumes axisymmetry. The radial density profile is taken to be parabolic and is constrained by the line-average polarimeter density measurement. Internal magnetic field probe measurements were not available during polarimeter shots, so the toroidal field also had to be modelled. From previous shots with an inserted magnetic probe array, the magnetic axis (i.e., peak toroidal field) is located at about the midpoint between the two electrodes, $r = 0.41$m. In addition, the ratio of the surface probe peak axial field to the magnetic axis peak toroidal field is approximately constant. This ratio is measured to be B_θ(axis)/B_z(wall) = 2.0 ± 0.2 using data from 9 shots. The toroidal field at the magnetic axis is modelled by taking the surface probe axial field and multiplying it by this ratio. The toroidal field profile can then be estimated by assuming a parabolic profile centred at the

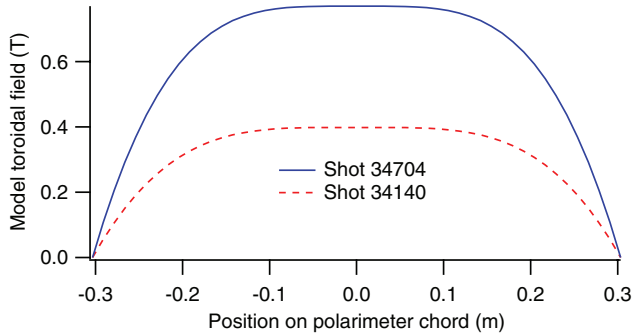

FIG. 7. Model toroidal field profile along polarimeter chord for shots 34140 and 34704 at the 352 axial position. The electrodes are located at polarimeter chord positions −0.31 m and 0.31 m, and the magnetic axis at 0 m.

magnetic axis and decreasing to zero at the walls. Figure 7 shows model toroidal field profiles.

The observed magnetic geometry matches well with a Grad-Shafranov model $\nabla \times \mathbf{B} = \lambda(\Psi)\mathbf{B}$. The eigenvalue λ is a function only of the poloidal flux function, Ψ, and has a linear profile of the form $\lambda(\Psi) = \bar{\lambda}[1 + \alpha(2\Psi/\Psi_{\max} - 1)]$, where $\bar{\lambda}$ is the average value of λ and α is a slope parameter that yields a peaked λ profile for positive values of α and a hollow λ profile for negative values. Configurations with a ratio $B_\theta(\text{axis})/B_z(\text{wall}) = 2.0 \pm 0.2$ correspond to peaked λ profiles with $\alpha = 0.6 \pm 0.1$. This is consistent with a decaying spheromak.[4]

Figure 8 compares model to measured Faraday rotation for typical shots before and after calibration. Measurements

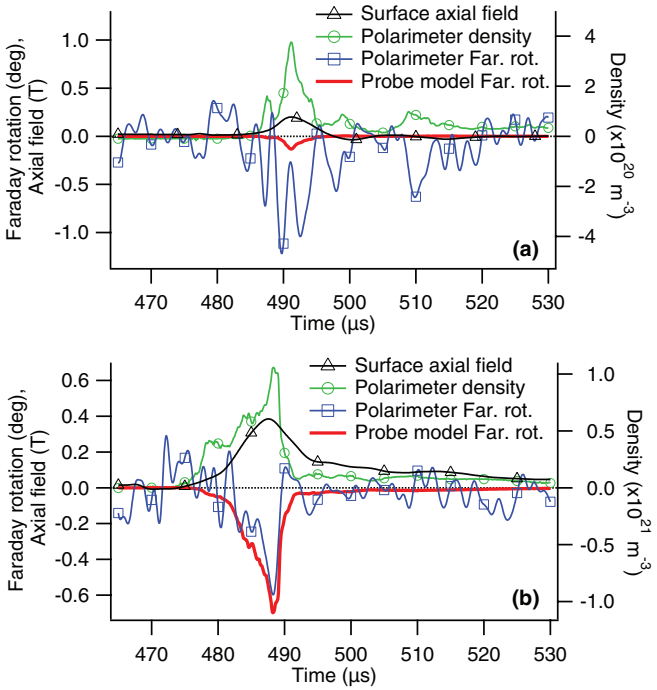

FIG. 8. Measured Faraday rotation compared to expected Faraday rotation from model toroidal field and density profiles. Signal bandwidths are 5 MHz for polarimeter density and 0.5 MHz for Faraday rotation and surface magnetic field. (a) Shot 34140: Poorly aligned beams produce Faraday rotation measurement that does not agree with model. (b) Shot 34704: Beam alignment error significantly reduced. Faraday rotation measurement agrees well with model.

before beam alignment agree poorly with the model. The large Faraday rotation at low density suggests fields in the tens of teslas, which is larger than what is possible from the measured accelerator currents. Also, the probe array has never measured fields of this magnitude at the 352 position on similar shots.

Pre-alignment measurements are also sometimes characterized by a sustained positive Faraday rotation. Given the known direction of the plasma toroidal magnetic field, the laser beam's direction of travel through the plasma, and the handedness of the circularly polarized plasma beams, the Faraday rotation signal should be predominantly negative. Therefore, signals with long periods of positive Faraday rotation are unlikely to be good measurements since this would require a sustained toroidal field in the direction opposite the expected one.

Results after the improved beam alignment are in good agreement with the model. The calibrated polarimeter generally produces Faraday rotation measurements in the correct direction with a magnetic field on the order of a tesla, which is typical of what is observed on magnetic probes. The error between the model and measurement is less than 0.3° at 0.5 MHz bandwidth. Discrepancies can primarily be attributed to capacitor discharge noise at early times and limitations of the model.

In order to evaluate the axial resolution, δz, of polarimeter Faraday rotation measurements, the spheromak's length and speed must be estimated from surface probe axial fields. The spheromak's axial length, L_{sph}, is taken as the full-width-half-maximum (FWHM) of the spline-fit to surface probe axial fields at the time of the maximum Faraday rotation signal (see Figure 9). The spheromak's speed, v_{sph}, is L_{sph} divided by the amount of time it is observed at the polarimeter's axial position, which is measured as the FWHM of the poloidal surface probe signal (as in Figure 8). The polarimeter's axial resolution is defined as $\delta z = v_{\text{sph}}/f_{\text{BW}}$ where f_{BW} is the polarimeter measurement bandwidth.

At the 352 position, v_{sph} ranges from 30 km/s to 150 km/s. Therefore, with $f_{\text{BW}} = 0.5$ MHz for Faraday rotation measurements, δz is between 6 cm and 30 cm. Typically, L_{sph} is between 0.75 m and 2 m, meaning the number of resolvable scale lengths $L_{\text{sph}}/\delta z$ ranges from 2.5 to 33. For shot 34704, the 1.0 m-long spheromak passes the 352 position at 100 km/s, suggesting the polarimeter can resolve 5 scale lengths across the spheromak.

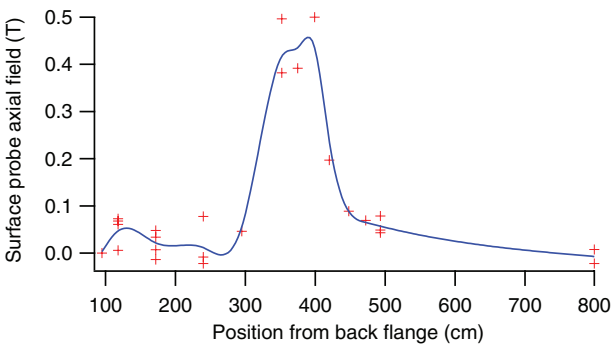

FIG. 9. Spline-fit to surface magnetic probe axial field measurements for shot 34704 at time of peak polarimeter Faraday rotation (488 μs).

VIII. SUMMARY AND FUTURE WORK

A three-beam heterodyne polarimeter using a CO_2 laser has been built at GF. The polarimeter beams are calibrated for polarization ellipticity and beam collinearity. Preliminary Faraday rotation measurements have been compared against a model and show a maximum error of 0.3° at 0.5 MHz bandwidth. The error is due to electrical noise and limitations of the model. With 0.5 MHz bandwidth, the polarimeter has an axial resolution between 6 cm and 30 cm depending on the speed of the spheromak.

In future upgrades, additional chords will be added to the system to improve polarimeter estimates of spatially resolved density and magnetic field. The polarimeter will be a valuable asset in better understanding spheromak behaviour.

ACKNOWLEDGMENTS

The authors acknowledge the Natural Sciences and Engineering Research Council of Canada and General Fusion, Inc., for financial support. Thanks to Roger J. Smith (University of Washington) and David Brower (UCLA) for helpful discussions.

[1]M. Laberge, J. Fusion Energy **28**, 179 (2009).
[2]S. Howard, M. Laberge, L. McIlwraith, D. Richardson, and J. Gregson, J. Fusion Energy **28**, 156 (2009).
[3]P. Bellan, *Spheromaks* (Imperial College Press, 2000).
[4]T. R. Jarboe, Phys. Plasmas **12**, 058103 (2005).
[5]C. D. Cothran, A. Falk, A. Fefferman, M. Landreman, M. R. Brown, and M. J. Schaffer, Phys. Plasmas **10**, 1748 (2003).
[6]W. X. Ding, D. L. Brower, S. D. Terry, D. Craig, S. C. Prager, J. S. Sarff, and J. C. Wright, Phys. Rev. Lett. **90**, 035002 (2003).
[7]S. E. Segre, Plasma Phys. Controlled Fusion **41**, R57 (1999).
[8]F. Chen, *Introduction to Plasma Physics and Controlled Fusion* (Plenum Press, 1984).
[9]I. Hutchinson, *Principles of Plasma Diagnostics* (Cambridge University Press, 2002).
[10]G. Dodel and W. Kunz, Infrared Phys. **18**, 773 (1978).
[11]D. L. Brower, W. X. Ding, S. D. Terry, J. K. Anderson, T. M. Biewer, B. E. Chapman, D. Craig, C. B. Forest, S. C. Prager, and J. S. Sarff, Rev. Sci. Instrum. **74**, 1534 (2003).
[12]T. Akiyama, S. Tsuji-Iio, R. Shimada, K. Nakayama, S. Okajima, M. Takahashi, K. Terai, K. Tanaka, T. Tokuzawa, and K. Kawahata, Rev. Sci. Instrum. **74**, 2695 (2003).
[13]Y. Jiang, D. L. Brower, L. Zeng, and J. Howard, Rev. Sci. Instrum. **68**, 902 (1997).
[14]W. X. Ding, D. L. Brower, W. F. Bergerson, and L. Lin, Rev. Sci. Instrum. **81**, 10D508 (2010).
[15]L. Lin, W. X. Ding, and D. L. Brower, Rev. Sci. Instrum. **83**, 10E320 (2012).
[16]M.-H. Kim, V. Kurz, G. Acbas, C. T. Ellis, and J. Cerne, J. Opt. Soc. Am. B **28**, 199 (2011).
[17]K. Guenther and JET-EFDA Contributors, Plasma Phys. Controlled Fusion **46**, 1423 (2004).